

# Two Paralleled Four Quadrant DC Chopper for Gradient Coil Magnetic Fields in MRI System

Hyung-Beom Park\* · Sang-Pil Mun · Han-Seok Park · Kyung-IL Woo\*\*

## Abstract

This paper presents a two-paralleled four quadrant DC chopper type PWM power conversion circuit in order to generate a gradient magnetic field in the Magnetic Resonance Imaging (MRI) system. This circuit has 8-IGBTs at their inputs/outputs to realize further high-power density, high speed current tracking control, and to get a low switching ripple amplitude in a controlled current in the Gradient Coils (GCs). Moreover, the power conversion circuit has to realize quick rise/fall response characteristics in proportion to various target currents in GCs. It is proposed in this paper that a unique control scheme can achieve the above objective DSP-based control system realize a high control facility and accuracy. It is proved that the new control system will greatly enlarge the diagnostic target and improve the image quality of MRI.

Key Words : Two-Paralleled Four Quadrant DC Chopper, Gradient Coils(GCs), High Speed Current Tracking Control, Magnetic Resonance Imaging(MRI)

## 1. Introduction

The MRI systems need a medical office detecting a disease in early stages. It has good points which is possible to take any section picture in human body, unnecessary to give consideration to side effects for the X- ray. The MRI systems can get any image in human body, since the hydrogen in the body radiates radio waves from a resonance with changing magnetic fields [1]. To

realize high-speed imaging, the gradient power amplifiers require higher output power as well as quick rise/fall response capability [2-4].

Considering this backdrop, a new power conversion circuit for switch-mode gradient power amplifiers in MRI systems is proposed in this paper using a parallel connection of conventional four quadrant DC chopper circuits with IGBTs at their inputs/outputs, and a unique digital control scheme for the circuit on the basis of optimal control. Furthermore, preview digital control is introduced into the amplifier with a corrective control scheme applied to improve the control of GC current and attain robustness. The effectiveness of the above scheme is evaluated through computer-aided analysis.

\* Main author : Pukyong National University

\*\* Corresponding author : Professor in the Division of Electrical, Control Engineering of Pukyong National University

Tel : +82-51-629-6321, Fax : +82-51-629-6305

E-mail : cogging@pknu.ac.kr

Date of submit : 2009. 6. 15

First assessment : 2009. 6. 19

Completion of assessment : 2009. 11. 11

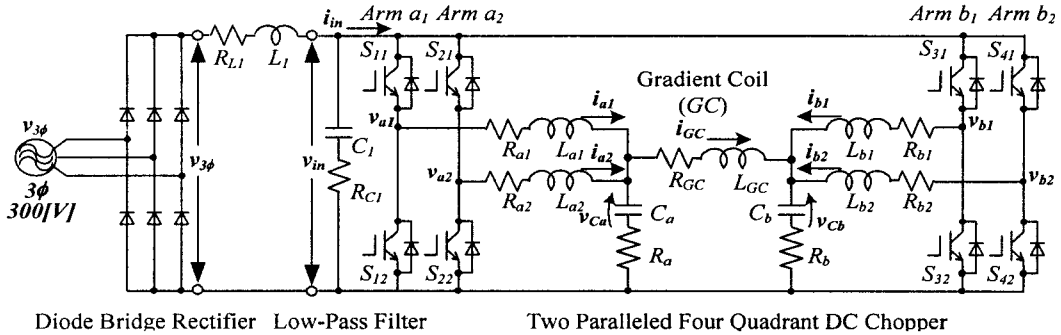


Fig. 1. The parallel connection four quadrant DC chopper circuit with IGBTs

## 2. Digital Control Scheme for Proposed Circuit

The discrete system state equation of the power conversion circuit shown in Fig. 1 can be written as

$$\begin{aligned} \mathbf{x}(k+1) &= \mathbf{A}\mathbf{x}(k) + \mathbf{B}\mathbf{u}(k-1) \\ \mathbf{y}(k) &= \mathbf{C}\mathbf{x}(k) \end{aligned} \quad (1)$$

where,

$\mathbf{x}(k) = [i_{a1}(k), i_{a2}(k), i_{b1}(k), i_{b2}(k), v_{ca}(k), v_{cb}(k), i_{GC}(k)]^T \in \mathbb{R}^{7 \times 1}$ , is the system state vector,  $\mathbf{u}(k-1) = [v_{a1} * p_1(k-1), v_{a2} * p_2(k-1), v_{b1} * p_3(k-1), v_{b2} * p_4(k-1)]^T \in \mathbb{R}^{4 \times 1}$  is the system input vector, and  $\mathbf{y}(k) = [i_{a1}(k), i_{a2}(k), i_{b1}(k), i_{b2}(k)]^T \in \mathbb{R}^{4 \times 1}$  is the system output vector. A, B, and C are real coefficient matrices with appropriate dimensions.

Since digital control involves a time lag, it is necessary for the DSPs to consider the calculating time. Therefore, the input signal  $u(k-1)$  is calculated between the sampling time  $k-1$  and  $k$ . The power switch devices are turned on and off so that the input voltages to each of the LCR filters are given some pulses with magnitude  $v_{in}$  or 0 and width  $p_i(k)$  ( $i=1$  to 4) centered during sampling interval  $T_s$ .

The pulse width vector  $\mathbf{p}(k) = [p_1(k), p_2(k), p_3(k), p_4(k)]^T \in \mathbb{R}^{4 \times 1}$  will be derived in terms of the following equation.

$$\mathbf{p}(k) = \frac{\mathbf{u}(k)}{v_{in}} \quad (2)$$

Although the same chopper inductor and capacitor as LC low pass filters are connected with each of the bridge arms, these are not effective enough to eliminate the current ripple. The basic concept of pulse generation procedure to minimize the current ripple is illustrated in Fig. 2. Using data sampled at  $t=(k-1)T_s$ , input vector  $u(k)$  is calculated during a sampling interval  $T_s$  with the pulses  $[p_1(k), p_3(k)]$  centered in the sampling interval  $T_s$  and the pulses  $[p_2(k), p_4(k)]$  equally divided in half and arranged on each side of the sampling interval  $T_s$ .

As a result of this pulse generation procedure, the filter inductor currents  $i_{La1}$  and  $i_{La2}$  (or  $i_{Lb1}$  and  $i_{Lb2}$ ) which take the form of triangular-waves are obtained as shown in Fig. 2. The ripples of filter inductor currents are mutually cancelled, and thus the ripple of the synthesized current  $i_{La1} + i_{La2}$  (or  $i_{Lb1} + i_{Lb2}$ ) becomes very small and its frequency is twice as high ( $2f_s$ ) as each of the inductor currents ( $f_s$ ). The current into the GC may be considered as been produced by the superposition of filter inductor currents  $i_{La1}$  and  $i_{La2}$  (or  $i_{Lb1}$  and  $i_{Lb2}$ ). However a small current will flow through the capacitor and in order to obtain better control of the GC current, it should be taken into consideration.

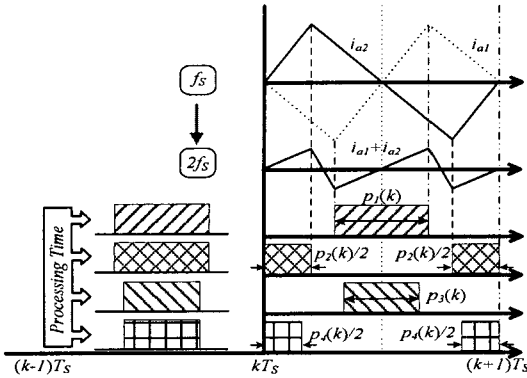


Fig. 2. IGBT gate signal layout in the amplifier

### 3. The Design of Optimal Control System

An error signal vector  $e(k) \in R^{4 \times 1}$  is defined as  $e(k) = y_{ref}(k) - y(k)$  where  $y_{ref}(k) \in R^{4 \times 1}$  consists of the output reference signals. Even though the GC current is designed as the combination of two target currents,  $y_{ref}$ , the GC current will not achieve the desired value since a current flows through the capacitor  $C_a(C_b)$ . Hence, in order to overcome this error, a corrective expression is added as

$$\begin{aligned} e_c(k) &= y_{ref}(k) + R_c(k) - y(k) \\ &= y_{ref,c}(k) - y(k) \end{aligned} \quad (3)$$

where,  $R_c(k) = F_c(k)x(k)$

$$F_c(k) = \begin{bmatrix} c_1(k) & 0 & 0 & 0 & 0 & 0 & 0 \\ 0 & c_1(k) & 0 & 0 & 0 & 0 & 0 \\ 0 & 0 & c_2(k) & 0 & 0 & 0 & 0 \\ 0 & 0 & 0 & c_2(k) & 0 & 0 & 0 \end{bmatrix}$$

$$c_1(k) = \frac{i_{La1}(k) + i_{La2}(k) - i_{Lgc}(k)}{2.0 \times (i_{La1}(k) + i_{La2}(k))}$$

$$c_2(k) = \frac{i_{Lb1}(k) + i_{Lb2}(k) + i_{Lgc}(k)}{2.0 \times (i_{Lb1}(k) + i_{Lb2}(k))}$$

$R_d(k)$  makes compensation for capacitor current

losses of each filter. Since  $R_d(k)$  is calculated each sampling time,  $e_c(k)$  deals with the difference between each filter current and reference, as usual.

In the design stages, we must take the processing delay time into account and compensate it. Assuming that the processing time, which is regarded as input delay time, is equal to a sampling interval  $T_s$ . The error system is derived from eq.(3).

$$\begin{bmatrix} e_c(k+1) \\ x(k+1) \\ u(k) \end{bmatrix} = \begin{bmatrix} I_4 & -CA & -CB \\ 0 & A & B \\ 0 & 0 & 0 \end{bmatrix} \begin{bmatrix} e_c(k) \\ x(k) \\ u(k-1) \end{bmatrix} + \begin{bmatrix} 0 \\ 0 \\ I_4 \end{bmatrix} u(k) + \begin{bmatrix} I_4 \\ 0 \\ 0 \end{bmatrix} y_{ref,c}(k+1) \quad (4)$$

$$X_D(k+1) = X_D(k) + G \Delta u(k) + G_R \Delta y_{ref,c}(k+1)$$

where,  $\Delta$  refers to the difference between the values corresponding to the present sampling time with that of the preceding sampling time.

A performance index J is defined as follows :

$$\begin{aligned} J = \sum_{k=1}^{\infty} \left\{ \begin{bmatrix} X_0^T(k) & \Delta u^T(k-1) \end{bmatrix} \begin{bmatrix} Q & 0 \\ 0 & 0 \end{bmatrix} \begin{bmatrix} X_0(k) \\ \Delta u(k-1) \end{bmatrix} \right. \\ \left. + \Delta u^T(k) H \Delta u(k) \right\} \end{aligned} \quad (5)$$

where,  $Q \in R^{11 \times 11}$  and  $H \in R^{4 \times 4}$  are the weighting factor matrices. According to optimal regulator theory,  $\Delta u(k)$  is derived by solving eq.(4), such that eq.(5) is minimized.

Since the futuristic reference values are known a priori, a preview control term is added to improve the overall response of the control system. On the basis of eq.(6), the improved digital optimal system is illustrated in Fig. 3.

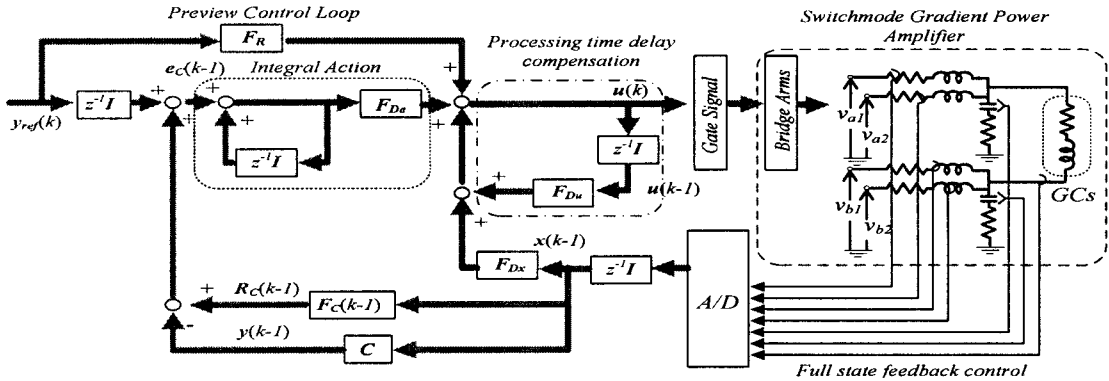


Fig. 3. Improved digital optimal base preview control system in the proposed two paralleled bridges power conversion PWM amplifier circuit

$$\begin{aligned}
 \Delta u(k) &= F_D X_D(k) + F_{DR} \Delta R(k+1) \\
 &= F_{De} e_C(k) + F_{Dx} \Delta x(k) \\
 &\quad + F_{Du} \Delta u(k-1) + F_{DR} \Delta y_{ref_c}(k+1) \\
 F_D &= -[H + G^T P G]^{-1} G^T P \Phi [\Phi G] \\
 &= F_0 [\Phi G] \\
 F_{DR} &= F_0 G_R \\
 P &= Q + \Phi^T P \Phi - \Phi^T P G [H + G^T P G]^{-1} G^T P K
 \end{aligned} \tag{6}$$

#### 4. Simulation Result and Their Discussions

The IGBTs now in use have a maximum operating frequency of about 20[kHz] that will maintain its stability.

Even though it is lower than devices such as MOSFETs or SITs its power levels are over 1,000[V]/100[A].

The circuit and control technique to overcome the disadvantage of low speed has been already described in this paper. As a result, IGBTs will be more suitable for practical power applications with high-speed operation. The simulation specifications are given in Table 1.

The parasitic resistors find each of the filter inductors which have various values from 0.05 to 0.1[Ω]. It is our intention to have different

performance characteristics for the 2-bridge modules connected in parallel.

If the filter inductor current control scheme is not carried out successfully, heavy currents will flow through the bridge circuits. Fig. 4 shows the simulation results when a sinusoidal-wave is inputted as the reference signal ( $y_{ref}$ ).

Table 1. Design Specifications and Circuit Parameters

Three-phase power source voltage	3F	300[V]
Sampling frequency	fs	20.0[kHz]
Gradient coil	Inductance	$L_{GC}$ 200[mH]
	Resistance	$R_{GC}$ 0.1[Ω]
Four quadrant chopper	Inductance	$L_a \sim L_b$ 180[mH]
	Capacitance	$C_a, C_b$ 5.0[mF]
	Resistance	$R_{Ca}, R_{Cb}$ 1.0[Ω]

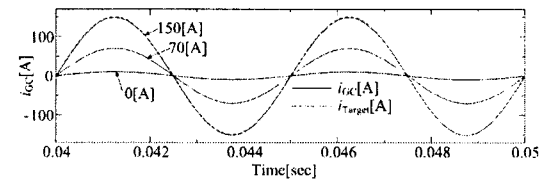


Fig. 4. Simulation results under sinusoidal pattern current tracking control scheme in MRI systems

The current into the GC is with a frequency of 200[Hz] and a peak of 150[A](300[A<sub>p-p</sub>]).

Furthermore, Fig. 5 shows GC current spectrums when using control schemes of Fig. 3.

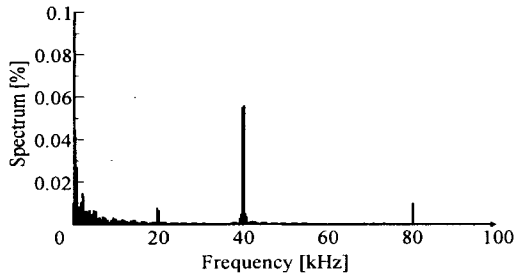


Fig. 5. Current spectrum in GCs under improved digital control scheme

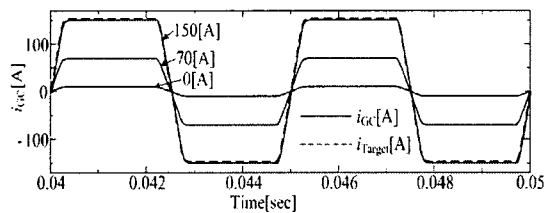
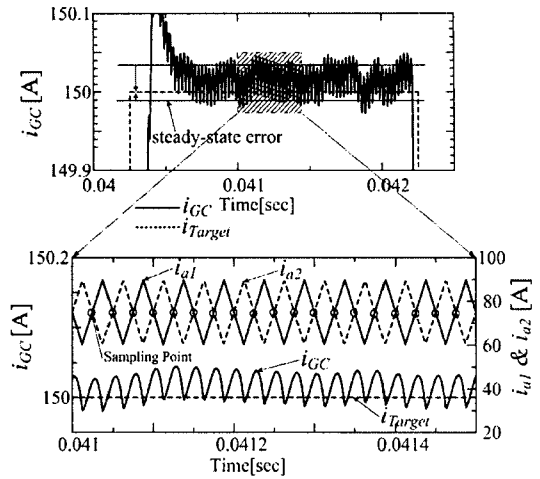


Fig. 6. Simulation results under trapezoidal pattern current tracking control scheme in MRI systems

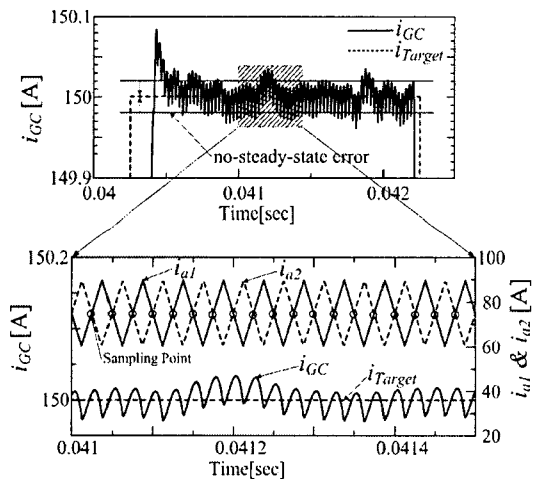
These figures show us that sinusoidal current wave forms could be controlled with fine shapes. A typical ramped-square wave current ( $i_{gc}$ ) with the frequency of 200[Hz] and a peak of 150[A](300[A<sub>p-p</sub>]) is next inputted into the GC. The simulation results are shown in Fig. 6.

It is confirmed that the rise/fall time of about 0.5[us] / 300[A] is achieved in 0.2 [mH]-GC. It can be seen that a significantly high GC-current tracking accuracy is achieved even while using sampled data every 20[kHz]. The distribution control scheme is carried out adequately as indicated in Fig. 7 since the filter inductor currents will be equal at all the sampling points.

As shown in this figure, an operating frequency that is double that of the IGBT's, that is 40[kHz], is achieved with a very small ripple amplitude on the flat-top of 150[A].



(a) Optimal preview control scheme



(b) Improved optimal preview control scheme

Fig. 7. Current waveforms of a each part

In case of controlled current with the correction term, the GC current has better control ability than with normal error systems. Normal systems have a large deviation of the mean value from the reference on the flat-top but whereas the improved system has no deviation at all. It is expected that the results shown in Fig. 4 to Fig. 7 will highly enlarge the diagnostic ability of MRI.

This consumption power is dissipated as a heat energy in MRI system. Fig. 8 gives the power loss

in proposed amplifier. Since the MRI system is expected to generate heat, we have to study how to eliminate the heat.

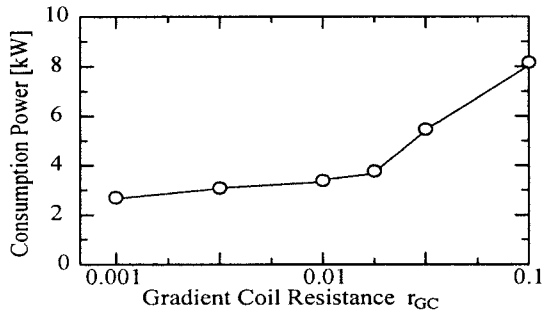


Fig. 8. Consumption power of the proposed amplifier

## 5. Conclusions

The PWM power conversion amplifier with two paralleled four quadrant DC chopper using IGBTs has been introduced into the switch-mode gradient power amplifiers in MRI systems in order to overcome the limitation of the low frequency switching characteristics and to obtain high output power levels. A unique digital control scheme to minimize the ripple and improve the rise/fall response characteristics of the output current in the GCs has also been proposed. It is a characteristic that the system state vectors have to be detected all at once at a given sampling time  $T_s$ . This fact also helps to simplify the current control scheme.

The simulation results through computer-aided analysis confirm that a high GC-current tracking accuracy is achieved under high power output levels in this system.

## References

- [1] K.P.Gokhale, A.Kawamura, and R.G.Hoft, "Dead Beat Microprocessor Control of PWM Inverter for Sinusoidal Output Waveforms Synthesis", IEEE-Trans. Industry Applications, pp. 901-910, 1987.
- [2] A.Kawamura, T.Haneyoshi, and R.G.Hoft, "Deadbeat Controlled PWM Inverter with Parameter Estimation Using Only Voltage Sensor", IEEE-Trans. Power Electronics, pp.118-125, 1988.
- [3] K.Siri and C.Q-Lee, "Current Distribution Control of Converters Connected in Parallel", Records of IEEE-IAS, pp.1274-1280, Oct. 1990.
- [4] Copley Controls Corp., "Extending the Scope of PWM Amplifiers", PCIM-Europe Magazine, pp.182-184, 1991

## Biography

### Hyung-Beom Park

He received the B.S, M.S. degrees in Electrical Engineering from Pukyong National University. He is currently in the Ph.D. course in Electrical Engineering from Pukyong National University. He is a managing director of the JUWON Engineering.

### Sang-Pil Mun

He Received B.S. degree in Electrical Engineering from Pukyong National University, Pusan, Korea in 1997 and M.S. and Ph.D. degrees in Electrical Engineering from Kyungnam University, Masan, Korea in 1999 and 2003 respectively. He was joined with the Electrical Energy Saving Research Center, Kyungnam University from 2003~2005 as a researcher. His research interests are in the areas of photovoltaic power generation systems, power electronics, soft-switching technology. He is a member of the KIEE, KIPE, KIIEE.

### Han-Seok Park

He received the B.S. and M.S. degrees in Electrical Engineering from Chung Ang University, Seoul, Korea in 1981 and 1983 and Ph.D. degree, in Electrical Engineering from Korea Maritime University, Pusan, Korea in 1996 respectively. He is currently a professor in the Division of Electrical, Control and Instrument Engineering of Pukyong National University. His research interests are energy conversion system and substitute energy system. He is a member of the KIEE, KIIEE, KOSME, KEEA.

### Kyung-IL Woo

He received the B.S, M.S., and Ph. D. degrees in Electrical Engineering from Hanyang University in 1995, 1997 and 2001 respectively. He is currently an associate professor in the Division of Electrical, Control and Instrument Engineering of Pukyong National University. His research interests are numerical analysis of electrical machines and control. He is a member of IEEE, KIEE, KIIEE.